JCB Report

Neurofilament heavy chain side arm phosphorylation regulates axonal transport of neurofilaments

Steven Ackerley, Paul Thornhill, Andrew J. Grierson, Janet Brownlees, Brian H. Anderton, P. Nigel Leigh, Christopher E. Shaw, and Christopher C.J. Miller

Departments of Neuroscience and Neurology, The Institute of Psychiatry, Kings College London, London SE5 8AF, UK

Neurofilaments possess side arms that comprise the carboxy-terminal domains of neurofilament middle and heavy chains (NFM and NFH); that of NFH is heavily phosphorylated in axons. Here, we demonstrate that phosphorylation of NFH side arms is a mechanism for regulating transport of neurofilaments through axons. Mutants in which known NFH phosphorylation sites were mutated to preclude phosphorylation or mimic permanent phosphorylation display altered rates of transport in a bulk transport assay. Similarly, application of roscovitine, an inhibitor of the NFH side arm kinase Cdk5/p35, accelerates neurofilament transport. Analyses of neurofilament movement in transfected living neurons demonstrated that a mutant mimicking permanent phosphorylation spent a higher proportion of time pausing than one that could not be phosphorylated. Thus, phosphorylation of NFH slows neurofilament transport, and this is due to increased pausing in neurofilament movement.

Introduction

Neurofilaments are transported through axons by a process termed slow axonal transport. However, recent studies have shown that they move at conventional fast rates of ~1 μm/s but that this movement is interrupted by prolonged pauses (Yabe et al., 1999; Prahlad et al., 2000; Roy et al., 2000; Shah et al., 2000; Wang et al., 2000; Wang and Brown, 2001). At any one time, most neurofilaments are therefore stationary, giving rise to an overall slow rate of transport.

The molecular mechanisms that regulate neurofilament transport are not properly understood, but a body of evidence associates increased phosphorylation of neurofilament side arms with slower transport rates (Ackerley et al., 2000; Sanchez et al., 2000; Yabe et al., 2001). In most mature neurons, neurofilaments comprise three subunit proteins, neurofilament light, middle, and heavy chains (NFL, NFM, and NFH),* and the carboxy-terminal domains of NFM and NFH form side arms that extend from the filament. These NFM/NFH side arms are phosphorylated in axons, with that of NFH being particularly heavily phosphorylated (Pant et al., 2000). Much of this phosphate is located in a domain that contains repeats of the motif lys-ser-pro (KSP). Kinases that phosphorylate the serines in these KSPs include Cdk5/p35, GSK-3α/β, and members of the MAPK/SAPK family (Pant et al., 2000). Here, we have investigated the role of side arm phosphorylation in neurofilament transport by analyzing movement of EGFP-tagged phosphorylation mutants of NFH in neurons. Our results provide direct experimental evidence to support a role for NFH side arm phosphorylation as a regulator of neurofilament transport.

Results and discussion

GFP–NFH coassembles with NFL and NFM, and phosphorylation of GFP–NFH mimics that of endogenous NFH in neurons

We confirmed that amino-terminal tagging of NFH with GFP does not influence its ability to form neurofilaments by studying its assembly properties in SW13− cells that do not contain intermediate filaments. Transfection of GFP-tagged wild-type NFH (GFP–NFHwt) or phosphorylation mutants of NFH (GFP–NFHala and GFP–NFHasp) with NFL, NFL + NFM, and NFL + NFM + NFH into SW13− cells all led to the formation of neurofilament networks that were not noticeably different from those formed by wild-type, untagged NFH (unpublished data; Fig. 1, A–F). Transfected GFP–NFHwt, GFP–NFHala, and GFP–NFHasp also colocalized with endogenous neurofilaments in rat

S. Ackerley, P. Thornhill, and A.J. Grierson contributed equally to this work.

Address correspondence to Christopher C.J. Miller, Department of Neuroscience, P.O. Box PO37, The Institute of Psychiatry, Denmark Hill, London SE5 8AF, UK. Tel.: 44-207-848-0393. Fax: 44-207-708-0017. E-mail: chris.miller@iop.kcl.ac.uk

*Abbreviations used in this paper: NFH, neurofilament heavy chain; NFL, neurofilament light chain; NFM, neurofilament middle chain; scg, superior cervical ganglion.

Key words: neurofilament proteins; axonal transport; amyotrophic lateral sclerosis; Alzheimer's disease; Cdk5/p35

The Journal of Cell Biology, Volume 161, Number 3, May 12, 2003 489–495
http://www.jcb.org/cgi/doi/10.1083/jcb.200303138

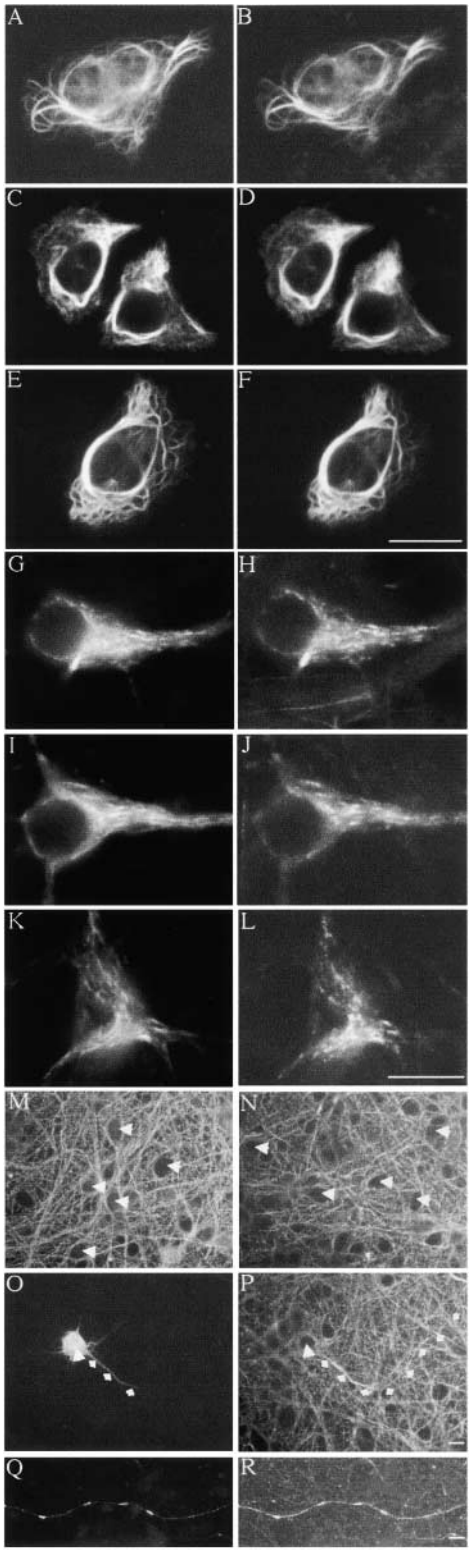

Figure 1. **GFP–NFH assembly and phosphorylation mimics that of endogenous NFH.** (A–F) SW13− cells transfected with NFL + NFM + NFH + either GFP–NFHwt (A and B), GFP–NFHala (C and D), or GFP–NFHasp (E and F). (G–L) Cortical neurons transfected with GFP–NFHwt (G and H), GFP–NFHala (I and J), or GFP–NFHasp (K and L). GFP–NFH was detected via the GFP tag in A, C, E, G, I, and K. NFL was detected using antibody NR4 in B, D, F, H, J, and L. A–L were visualized 16 h after transfection, but similar images of cortical neurons were obtained at earlier (140–260 min) and later (48 h) times. (M and N) Cortical neurons stained with antibodies 8D8 (M) and RT97 (N); unstained cell bodies are arrowed. (O–R) Cortical neurons transfected with GFP–NFHwt and costained with RT97. O and P are visualized 200 min after transfection, and Q and R are visualized 48 h after transfection. O and Q show GFP–NFHwt via the GFP tag; P and R show RT97 labeling. Large arrow shows cell body, and small arrows show trace axon of a transfected cell. Note the increased RT97 labeling in regions of axons where GFP–NFHwt is present, but also note the absence of RT97 labeling in cell bodies. Bars, 20 μm.

cortical neurons (Fig. 1, G–L). These results are in agreement with earlier studies of GFP–NFH/M (Ackerley et al., 2000; Roy et al., 2000; Wang et al., 2000).

NFH and NFM side arms are heavily phosphorylated in axons but not cell bodies. Thus, antibodies 8D8 and RT97, which detect phosphorylated NFH/NFM side arms, and antibody RMO45, which detects phosphorylated NFM side arms, all labeled axons but not cell bodies in cortical neurons (Fig. 1, M and N, 8D8 and RT97). Labeling of axons with RT97 commenced ~20 μm from cell bodies, which was determined by analyzing RT97 and NA1211 dual-labeled neurons; NA1211 detects NFH irrespective of its phosphorylation status. These results are consistent with earlier analyses of NFM/H phosphorylation in cortical neurons (Ackerley et al., 2000; Brownlees et al., 2000).

Transfection of GFP–NFHwt, GFP–NFHala, or GFP–NFHasp did not alter this RT97/8D8 labeling pattern over the time periods in which GFP–NFH transport was investigated (140–260 min and 48 h after transfection, see below); cell bodies remained negative and axons positive for RT97/8D8. Furthermore, regions of axons that contained GFP–NFHwt showed increased RT97/8D8 staining, which shows that phosphorylation of the GFP–NFH species on these epitopes is mimicking that of endogenous NFH (unpublished data; Fig. 1, O–R).

At least some serines within KSP repeats 44–48, 50, and 51 of NFH are targeted by Cdk5/p35

Most phosphorylation sites in NFH side arm are within a domain that contains repeats of the motif KSP (Fig. 2 A), but only 12 of these have been formally identified as in vivo phosphorylation sites in the rat (Elhanany et al., 1994). KSPs with the motif KSPXK are believed to be targeted by Cdk5/p35, and several lines of evidence indicate that these are functionally significant (Shetty et al., 1993; Guidato et al., 1996; Sun et al., 1996; Bajaj and Miller, 1997). We therefore chose to analyze the effect of Cdk5/p35 phosphorylation on NFH transport. The known in vivo phosphoserines within the consensus Cdk5/p35 motif are those in repeats 44–48, 50, and 51 (Elhanany et al., 1994), and these were mutated to alanine to preclude phosphorylation or aspartate to mimic permanent phosphorylation (Fig. 2 A). There are many examples where the substitution of such a charged residue accurately mimics the functional effect of phosphorylation (Eidenmuller et al., 2000).

Transfection of NFHwt alone into COS cells revealed that it had an accelerated rate of migration on SDS-PAGE compared with hyperphosphorylated NFH from brain when blots were probed with antibody NA1211 (Fig. 2 B). However, cotransfection with Cdk5/p35 induced a shift in a pro-

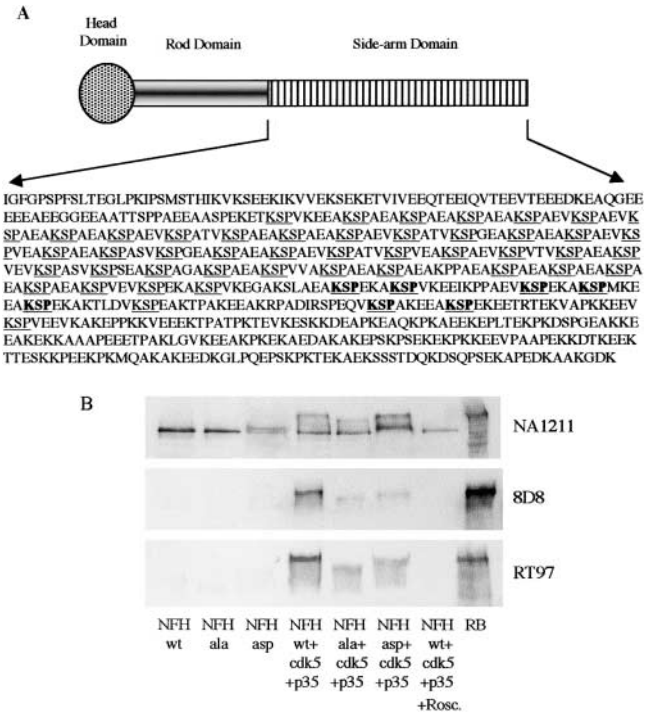

Figure 2. **Structure and phosphorylation of rat NFH by Cdk5/p35.** (A) Schematic of rat NFH with KSP sites underlined and mutated sites shown in bold. (B) Phosphorylation of NFHwt, NFHala, and NFHasp by Cdk5/p35 in transfected COS cells. Cells were transfected with NFHwt, NFHala, or NFHasp ± Cdk5/p35 as indicated, and the samples were probed on immunoblots with antibodies NA1211, 8D8, and RT97. RB is a sample of rat brain. 8D8 and RT97 both recognize phosphorylated NFH side arms; NA1211 is an NFH phosphorylation-independent antibody. Roscovitine (Rosc.) was applied 16 h before harvesting.

portion of transfected NFHwt so that it migrated close to NFH from brain; this shift was abolished in cells treated with the Cdk5/p35 inhibitor roscovitine (Fig. 2 B). Similarly, cotransfection of NFHwt with Cdk5/p35 increased its reactivity with antibodies, 8D8 and RT97, that detect phosphorylated NFH side arms (Fig. 2 B), which is in agreement with several previous studies (Guidato et al., 1996; Sun et al., 1996; Bajaj and Miller, 1997).

Mutant NFH in which the Cdk5/p35 sites were mutated to alanine (NFHala) comigrated with NFHwt when transfected alone into COS cells, but mutation of the sites to aspartate (NFHasp) induced a minor upward shift in a proportion of the transfected protein. This may be due to the aspartate residues mimicking phosphorylation that primes phosphorylation on other residues to induce a shift. NFHala and NFHasp did not react or reacted only weakly with antibodies 8D8 and RT97. However, after cotransfection of the mutants with Cdk5/p35, increased labeling with antibodies 8D8 and RT97 was observed; although this was significantly weaker than NFHwt in Cdk5/p35-cotransfected cells (Fig. 2 B). Cotransfection of NFHala or NFHasp with Cdk5/p35 also induced upward mobility shifts in a proportion of the transfected protein. However, the shift for NFHala was minor, whereas that for NFHasp was more pronounced so that it migrated close to NFH from brain. These results are consistent with the notion that some, if not all, of the sites mutated in NFHala are phosphorylated by Cdk5/p35 but that Cdk5/p35 targets other, as yet unidentified, sites.

The failure of NFHasp to react strongly with 8D8 and RT97 is as expected. Substituting charged residues in tau mimics the functional effects of phosphorylation but does not generate the epitopes for phosphorylation-dependent antibodies (Eidenmuller et al., 2000).

Mutation of NFH phosphorylation sites and inhibition of Cdk5/p35 alters NFH transport rates in a bulk transport assay

We calculated the transport rate of NFHwt, NFHala, and NFHasp in axons using a previously described assay (Ackerley et al., 2000). GFP–NFHwt was transported at a rate of ~80 μm/h, and this was not significantly different from that of GFP–NFM (Fig. 3 A). These rates were linear over the course of the experiment, which suggests that very early movement of nonphosphorylated neurofilaments close to cell bodies (Sanchez et al., 2000) is not being studied. Indeed, dual labeling of GFP–NFHwt-transfected cells with RT97 revealed that phosphorylation on NFH to generate this epitope commences ~20 μm from the cell body (Fig. 1, O and P). This is less than the distance travelled by GFP–NFHwt/ala/asp at the first time point analyzed (Ackerley et al., 2000; Fig. 3, legend).

We next examined how the mutation of phosphorylation sites affects NFH transport. GFP–NFHasp was transported significantly slower (52 μm/h) and GFP–NFHala significantly faster (108 μm/h) than GFP–NFHwt (Fig. 3 B). GFP–NFHala transport was determined for the first four time points, because at later times, its signal became progressively weaker toward the front, which precluded accurate measurements. The weaker signal obtained from GFP–NFHala at these later time points is consistent with the more rapid transport of a finite amount of GFP–NFHala with a concomitant dilution of fluorescent signal.

We also calculated the average distance moved by GFP–NFHwt and GFP–NFHasp 240 min after transfection in the presence of the Cdk5/p35 inhibitor roscovitine. Cdk5/p35 is active in cortical neurons (Nikolic et al., 1996). 20 μM roscovitine or vehicle was applied to the cells 130 min after transfection and maintained throughout the course of the experiment. Roscovitine did not induce any noticeable changes in the cells, including alterations to nuclear morphology. However, roscovitine significantly increased the distance travelled by GFP–NFHwt at this time point but had little effect on GFP–NFHasp (Fig. 3 C). Thus, mutation of Cdk5/p35 sites in NFH to preclude or mimic permanent phosphorylation modulates NFH transport, and inhibition of Cdk5/p35 activity with roscovitine significantly accelerates NFH transport. For all of the above assays, three independent experiments were performed using different preparations of plasmid DNAs.

Mutation of NFH phosphorylation sites alters NFH transport properties in transfected living cortical neurons

Although neurofilaments move at an overall slow rate of transport, this is now known to be due to rapid movement

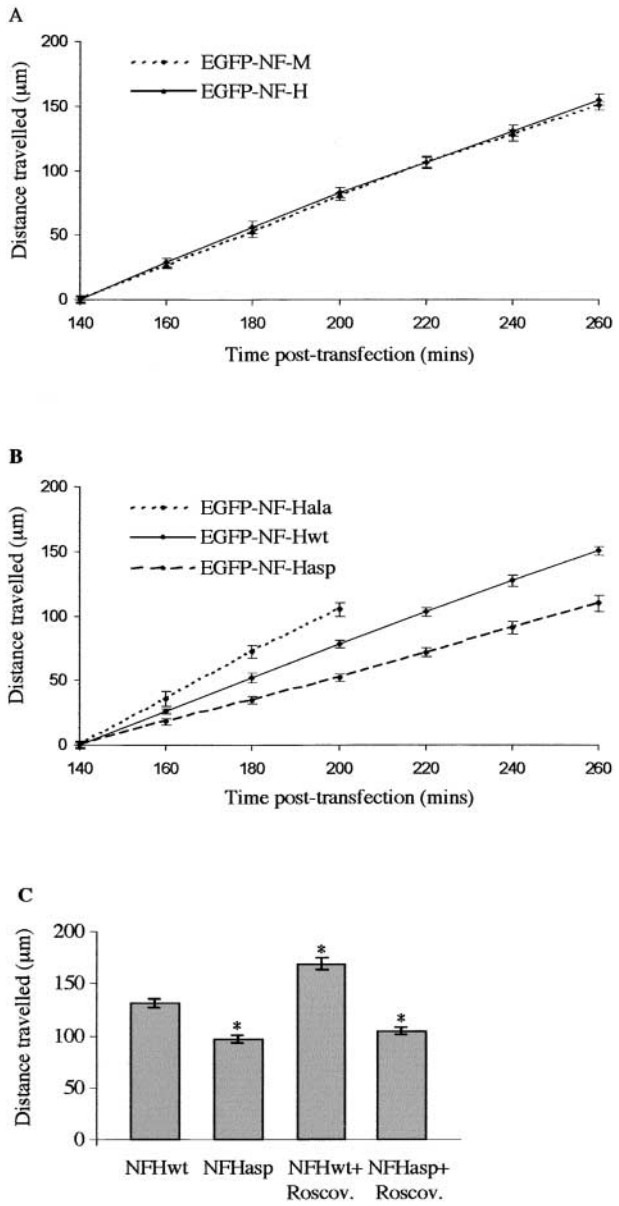

Figure 3. **Analyses of GFP–NFH transport in transfected neurons.** (A) Distances travelled by GFP–NFHwt and GFP–NFM at 140–260 min after transfection. One-way ANOVA tests showed no significant differences between GFP–NFHwt and GFP–NFM transport at any time point. (B) Distances travelled by GFP–NFHwt, GFP–NFHala, and GFP–NFHasp at 140–260 min after transfection. One-way ANOVA tests showed significant differences between GFP–NFHwt and GFP–NFHala ($P = 0.045$) and between GFP–NFHala and GFP–NFHasp ($P = 0.001$) at the 160-min time point. GFP–NFHwt and GFP–NFHasp displayed significant differences at the 180-min time point ($P = 0.005$). At later time points, significant differences between all three GFP–NFH proteins were observed ($P < 0.001$). (C) Histogram shows distance travelled by GFP–NFHwt and GFP–NFHasp 240 min after transfection in either 20 μM roscovitine (Roscov.) or vehicle-treated neurons. Roscovitine or vehicle was applied 130 min after transfection. An asterisk indicates treatments that display significant differences ($P < 0.001$) compared with vehicle-treated GFP–NFHwt, as analyzed by One-way ANOVA tests. No significant difference of GFP–NFHasp transport was observed between vehicle- and roscovitine-treated neurons. As detailed previously (Ackerley et al., 2000), the distances travelled by GFP–NFHwt/ala/asp at the first (140 min) time point are all adjusted to zero, so as to facilitate comparisons between experiments, and do not represent the actual distances travelled from cell bodies. Each data set shown for A–C is from one representative experiment, and error bars are the SEM.

that is interrupted by prolonged pauses. This has been revealed by analyses of GFP–NFM and GFP–NFH movement in transfected living superior cervical ganglion (scg) neurons (Roy et al., 2000; Wang et al., 2000). Scg neurons possess gaps in their axonal neurofilament network through which moving GFP–NFM/H can be visualized several days after transfection. We found that similar gaps in GFP–NFH fluorescence also appeared in the transfected cortical neurons 48 h after transfection (Fig. 4, A and B). These weaker areas of fluorescence enabled us to monitor neurofilament movement in a manner similar to that described for scg neurons.

To characterize GFP–NFHwt movement in cortical neurons, we acquired time-lapse movies from 20 transfected cells with the duration of observation ranging from 1.08 to 3.75 min. Moving fluorescent structures were defined as those that exhibited movement ≥0.3 μm in 5 s; pauses were thus any movement less than this. The length of GFP–NFHwt moving structures varied from 1.3 to 4.4 μm, and movement was bidirectional. The velocity of GFP–NFHwt movement, excluding any pauses, varied between 0.08 and 0.96 μm/s in the anterograde direction and between 0.08 and 0.93 μm/s in the retrograde direction, but pauses in movement were observed. These speeds and pausing characteristics are similar to those described for GFP–NFM and GFP–NFH in scg neurons (Roy et al., 2000; Wang et al., 2000). Examples of GFP–NFHwt movement are shown in Fig. 4, A–C (see Video 1, available at http://www.jcb.org/cgi/content/full/jcb.200303138/DC1).

NFH side arm phosphorylation is dynamic, but the phosphorylation states of GFP–NFHala and GFP–NFHasp on the seven sites investigated are defined irrespective of their subcellular location. We therefore compared the movement characteristics of these two mutants.

The lengths of GFP–NFHala and GFP–NFHasp moving fluorescent structures were not noticeably different from those of GFP–NFHwt, and their velocities, excluding pauses, were similar to GFP–NFHwt. The two mutants also exhibited bidirectional movement, but analyses of this revealed no significant differences. Because images of moving GFP–NFH and GFP–NFM reveal minipauses (Roy et al., 2000; Wang et al., 2000), we next considered whether GFP–NFHala and GFP–NFHasp displayed differences in pausing. Moving GFP–NFHala and GFP–NFHasp spent an average of 16 and 37% pausing, respectively, and statistical analyses revealed a significant difference. In a separate experiment, we also measured the total distances moved by GFP–NFHala and GFP–NFHasp per minute of microscope observation time. As the majority of neurofilaments are stationary at any one time, many movies do not show any movement. In this assay, GFP–NFHala moved significantly more than GFP–NFHasp. These results are summarized in Table I. Examples of GFP–NFHala and GFP–NFHasp movement and pausing are shown in Fig. 4 C.

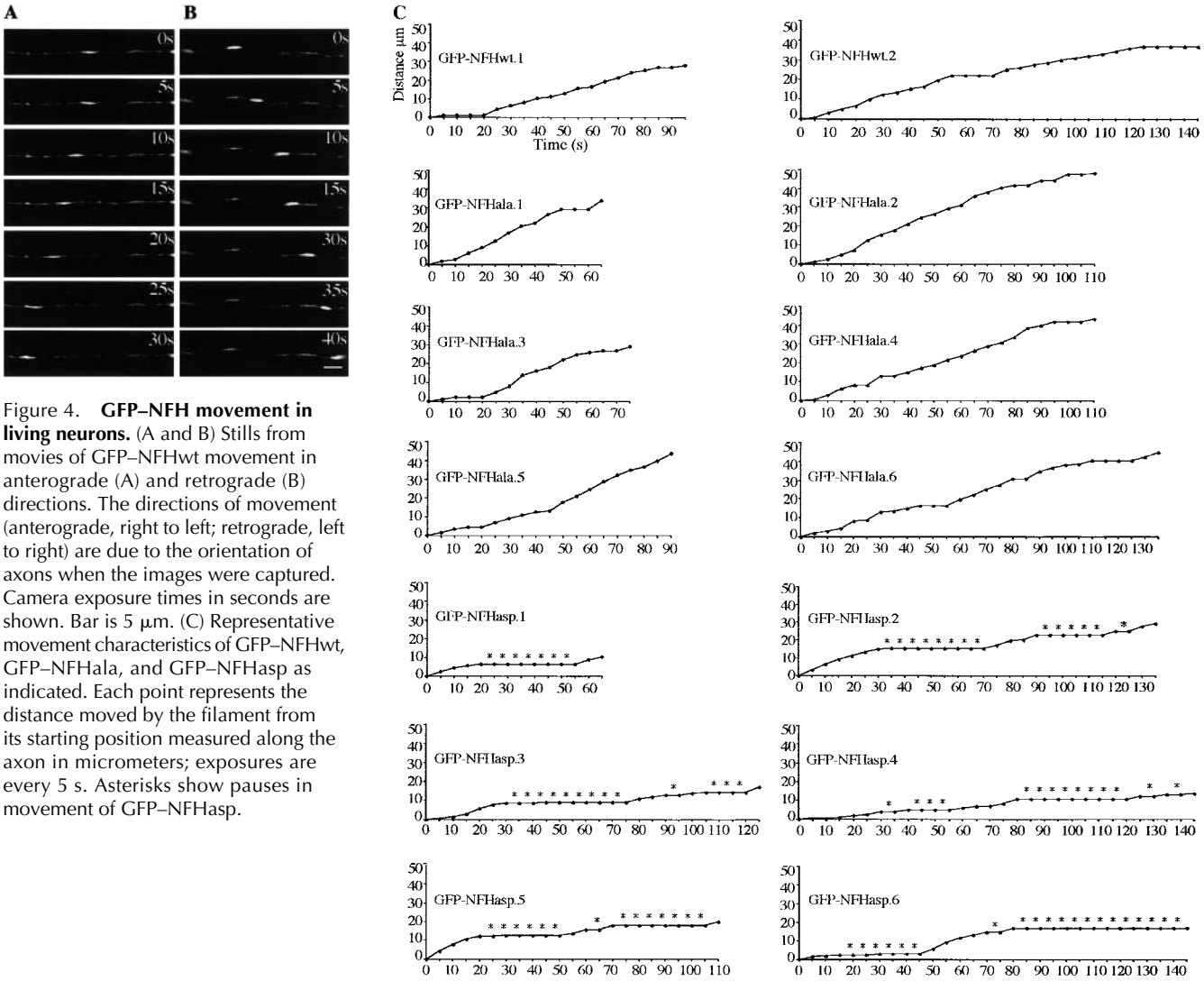

Figure 4. **GFP–NFH movement in living neurons.** (A and B) Stills from movies of GFP–NFHwt movement in anterograde (A) and retrograde (B) directions. The directions of movement (anterograde, right to left; retrograde, left to right) are due to the orientation of axons when the images were captured. Camera exposure times in seconds are shown. Bar is 5 µm. (C) Representative movement characteristics of GFP–NFHwt, GFP–NFHala, and GFP–NFHasp as indicated. Each point represents the distance moved by the filament from its starting position measured along the axon in micrometers; exposures are every 5 s. Asterisks show pauses in movement of GFP–NFHasp.

The role of NFH side arm phosphorylation is not properly understood, but a body of evidence suggests that it is a mechanism for regulating neurofilament transport (de Waegh et al., 1992; Ackerley et al., 2000; Sanchez et al., 2000; Yabe et al., 2001). Here, we have used mutants of NFH to investigate the role of phosphorylation in transport. Using a bulk transport assay, we demonstrate that mutants mimicking permanent phosphorylation are transported slower, and that mutants that cannot be phosphorylated move faster than wild-type NFH. In these assays, inhibition of Cdk5/p35 activity with roscovitine also accelerates neurofilament transport. In a second series of experiments, we

Table I. **Summary of movement characteristics of GFP–NFHala and GFP–NFHasp filaments in living cortical neurons**

Velocity of moving GFP–NFHala and GFP–NFHasp excluding pauses	No difference between GFP–NFHala and GFP–NFHasp. GFP–NFHala varied between 0.08 and 1.13 µm/s in the anterograde direction and between 0.08 and 1.27 µm/s in the retrograde direction; GFP–NFHasp varied between 0.08 and 1.1 µm/s in the anterograde direction and between 0.07 and 1.22 µm/s in the retrograde direction (analyzed by Mann-Whitney test).
Anterograde vs. retrograde movement of GFP–NFHala and GFP–NFHasp	No difference between GFP–NFHala and GFP–NFHasp (analyzed by chi-square test).
Pauses in movement of moving GFP–NFHala and GFP–NFHasp	GFP–NFHala pauses significantly less than GFP–NFHasp (16 vs. 37%; $P = 0.005$ by Mann-Whitney test).
Distance moved by GFP–NFHala and GFP–NFHasp per minute of microscope observation time	GFP–NFHala moves significantly more than GFP–NFHasp. GFP–NFHala moved a total of 8.64 µm/min of observation, whereas GFP–NFHasp moved 3.12 µm/min of observation ($P = 0.001$ by Mann-Whitney test).

GFP–NFHala movement was characterized from movies acquired from 27 cells, with the duration of observation ranging from 1 to 2.83 min; GFP–NFHasp movement was from 17 cells, with the duration of observation ranging from 1 to 2.83 min. Calculations of distance moved per minute of observation time were made from 37 GFP–NFHala- and 26 GFP–NFHasp-transfected cells viewed for a total of 60 and 40.42 min, respectively.

analyzed neurofilament movement in living neurons and demonstrate that mutation to mimic permanent phosphorylation significantly increases the proportion of time that neurofilaments spend pausing. Together, these data provide strong experimental evidence that NFH side arm phosphorylation is a regulator of neurofilament transport.

Very recently, Rao et al. (2002) created mice in which the side arm domain of NFH had been deleted by gene replacement. These animals show no alteration in neurofilament transport, which suggests that the side arm is not involved in this process. However, other transgenic studies have supported a role for NFH in neurofilament transport; ablation of the NFH gene accelerates neurofilament transport, and increased NFH expression inhibits transport (Collard et al., 1995; Marszalek et al., 1996; Zhu et al., 1998). Also, NFM and NFH phosphorylation states are intimately related; NFM phosphorylation is increased (including the RT97 epitope) in both NFH knockout and NFH side arm–deleted mice (Tu et al., 1995; Zhu et al., 1998; Sanchez et al., 2000; Rao et al., 2002). Thus, there are compensatory changes in NFM after modulation of NFH expression in mice, and these changes may well effect neurofilament transport.

The precise mechanisms by which phosphorylation inhibits neurofilament transport are not clear. One possibility is that phosphorylation leads to a detachment of neurofilaments from their motors. Alternatively, phosphorylation may influence neurofilament interactions with other axoplasmic components that somehow alter movement. The identification of neurofilament motors will enable a better understanding of this process.

Materials and methods

Plasmids

Expression plasmids for rat NFL, NFM, NFH, Cdk5, and p35 were previously described (Guidato et al., 1996; Ackerley et al., 2000). Amino-terminal GFP-tagged rat NFH was prepared by cloning the cDNA into pEGFP-C3 (CLONTECH Laboratories, Inc.).

Serines within KSP repeats 44–48, 50, and 51 of NFH side arm were mutated to either alanine or aspartate using a Chameleon mutagenesis kit (Stratagene) in three consecutive rounds. Serines in repeats 44 and 45 were mutated using oligonucleotides ATCTCTTCCTTCACAGGGGCCTTGGCCTTCTCAGGGGCCTTGGCCTCAGCTAGGGATTTTGCAC (ala) or ATCTCTTCCTTCACAGGGTCCTTGGCCTTCTCAGGGTCCTTGGCCTCAGCTAGGGATTTTGCAC (asp). Serines in repeats 50 and 51 were mutated using oligonucleotides CTGGTCTCTTCCTTCTCGGGGGCCTTGGCCTCCTCCTTGGCAGGAGCTTTGACCTGCTCAGGGGATCTGATGT (ala) and CTGGTCTCTTCCTTCTCGGGGTCCTTGGCCTCCTCCTTGGCAGGATCTTTGACCTGCTCAGGGGATCTGATGT (asp). Serines in repeats 46, 47, and 48 were mutated using oligonucleotides ATCCAGAGTCTTGGCCTTCTCAGGAGCCTTGGCCTCCTCCTTCATGGGGGCCTTGGCCTTCTCGGGGGCTTTCACCTCAGCTGGAGGCTTGAT (ala) and ATCCAGAGTCTTGGCCTTCTCAGGGTCCTTGGCCTCCTCCTTCATGGGGTCCTTGGCCTTCTCGGGGTCTTTCACCTCAGCTGGAGGCTTGAT (asp).

Cell culture and transfection

SW13− cells, COS cells, and cortical neurons were grown and transfected as previously described (Guidato et al., 1996; Ackerley et al., 2000). Roscovitine was obtained from Calbiochem and prepared as a 20 mM solution in DMSO.

Immunoblot and immunofluorescence analyses

COS cells were processed for SDS-PAGE and immunoblotting, and SW13− cells and neurons were fixed and immunostained as previously described (Ackerley et al., 2000). The primary antibodies used were NA1211 (Affiniti), NR4 (Sigma-Aldrich), 8D8, and RT97.

Axonal transport of GFP–NFH/NFM

Bulk axonal transport of GFP–NFM and GFP–NFH was analyzed in cortical neurons using a previously published method (Ackerley et al., 2000; Brownlees et al., 2002; Utton et al., 2002). Statistical analyses were performed using One-way ANOVA tests, and the rates of transport were calculated using linear regression analyses.

To study GFP–NFH movement in living neurons, cortical neurons were transfected as for the bulk transport assays and observed 48 h later using a Carl Zeiss MicroImaging, Inc. Axiovert S100 microscope and a 100× Fluar lens. Cells grown on coverslips were viewed in normal medium using an Open Perfusion Micro-Incubator equipped with bipolar temperature controller (models PDM1–2 and TC-202; Medical Systems Corp.) that was attached to the microscope stage. Cells were gassed with 5% CO_2. Images were captured from 1-s exposures taken every 5 s using a CCD camera (model RTE/CCD-1300-Y/HS; Princeton Instruments). The shutter was controlled using a motorized shutter controller (Lambda 10-2; Sutter Instruments). Filter sets for EGFP were from Chroma Technology Corp. Images were analyzed using Metamorph Software, and Quicktime movies were prepared using Adobe Premiere.

Only cells that exhibited a healthy appearance were monitored, and we did not acquire data from cells expressing high levels of GFP–NFH (as judged by brightness of fluorescence) because this can induce pathological changes (Roy et al., 2000). Statistical analyses of GFP–NFH movement in living transfected neurons were performed using chi-square, One-way ANOVA, and Mann-Whitney tests as indicated in the text.

Online supplemental material

The supplemental material (Video 1) is available at http://www.jcb.org/cgi/content/full/jcb.200303138/DC1. Video 1 is a Quicktime movie of GFP–NFHwt anterograde movement in a transfected cortical neuron. 1-s exposures were taken every 5 s.

We thank Ron Liem and Li-Huei Tsai for plasmids.

This work was supported by grants from the Medical Research Council, Wellcome Trust, UK Motor Neurone Disease Association, and Kings Healthcare Trust.

Submitted: 20 March 2003
Revised: 27 March 2003
Accepted: 27 March 2003

References

Ackerley, S., A.J. Grierson, J. Brownlees, P. Thornhill, B.H. Anderton, P.N. Leigh, C.E. Shaw, and C.C.J. Miller. 2000. Glutamate slows axonal transport of neurofilaments in transfected neurons. *J. Cell Biol.* 150:165–175.

Bajaj, N.P., and C.C.J. Miller. 1997. Phosphorylation of neurofilament heavy-chain side-arm fragments by cyclin-dependent kinase-5 and glycogen synthase kinase-3a in transfected cells. *J. Neurochem.* 69:737–743.

Brownlees, J., A. Yates, N.P. Bajaj, D. Davis, B.H. Anderton, P.N. Leigh, C.E. Shaw, and C.C.J. Miller. 2000. Phosphorylation of neurofilament heavy chain side-arms by stress activated protein kinase-1b/Jun N-terminal kinase-3. *J. Cell Sci.* 113:401–407.

Brownlees, J., S. Ackerley, A.J. Grierson, N.J. Jacobsen, K. Shea, B.H. Anderton, P.N. Leigh, C.E. Shaw, and C.C. Miller. 2002. Charcot-Marie-Tooth disease neurofilament mutations disrupt neurofilament assembly and axonal transport. *Hum. Mol. Genet.* 11:2837–2844.

Collard, J.-F., F. Cote, and J.-P. Julien. 1995. Defective axonal transport in a transgenic mouse model of amyotrophic lateral sclerosis. *Nature.* 375:61–64.

de Waegh, S.M., V.M.-Y. Lee, and S.T. Brady. 1992. Local modulation of neurofilament phosphorylation, axonal caliber and slow axonal transport by myelinating Schwann cells. *Cell.* 68:451–463.

Eidenmuller, J., T. Fath, A. Hellwig, J. Reed, E. Sontag, and R. Brandt. 2000. Structural and functional implications of tau hyperphosphorylation: information from phosphorylation-mimicking mutated tau proteins. *Biochemistry.* 39:13166–13175.

Elhanany, E., H. Jaffe, W.T. Link, D.M. Sheeley, H. Gainer, and H.C. Pant. 1994. Identification of endogenously phosphorylated KSP sites in the high-molecular-weight rat neurofilament protein. *J. Neurochem.* 63:2324–2335.

Guidato, S., L.-H. Tsai, J. Woodgett, and C.C.J. Miller. 1996. Differential cellular phosphorylation of neurofilament heavy side-arms by glycogen synthase kinase-3 and cyclin-dependent kinase-5. *J. Neurochem.* 66:1698–1706.

Marszalek, J.R., T.L. Williamson, M.K. Lee, Z.S. Xu, P.N. Hoffman, M.W.

Becher, T.O. Crawford, and D.W. Cleveland. 1996. Neurofilament subunit NF-H modulates axonal diameter by selectively slowing neurofilament transport. *J. Cell Biol.* 135:711–724.

Nikolic, M., H. Dudek, Y.T. Kwon, Y.F.M. Ramos, and L.H. Tsai. 1996. The cdk5/p35 kinase is essential for neurite outgrowth during neuronal differentiation. *Genes Dev.* 10:816–825.

Pant, H.C., Veeranna, and P. Grant. 2000. Regulation of axonal neurofilament phosphorylation. *Curr. Top. Cell. Regul.* 36:133–150.

Prahlad, V., B.T. Helfand, G.M. Langford, R.D. Vale, and R.D. Goldman. 2000. Fast transport of neurofilament proteins along microtubules in squid axoplasm. *J. Cell Sci.* 113:3939–3946.

Rao, M.V., M.L. Garcia, Y. Miyazaki, T. Gotow, A. Yuan, S. Mattina, C.M. Ward, N.A. Calcutt, Y. Uchiyama, R.A. Nixon, and D.W. Cleveland. 2002. Gene replacement in mice reveals that the heavily phosphorylated tail of neurofilament heavy subunit does not affect axonal caliber or the transit of cargoes in slow axonal transport. *J. Cell Biol.* 158:681–693.

Roy, S., P. Coffee, G. Smith, R.K.H. Liem, S.T. Brady, and M.M. Black. 2000. Neurofilaments are transported rapidly but intermittently in axons: implications for slow axonal transport. *J. Neurosci.* 20:6849–6861.

Sanchez, I., L. Hassinger, R.K. Sihag, D.W. Cleveland, P. Mohan, and R.A. Nixon. 2000. Local control of neurofilament accumulation during radial growth of myelinating axons in vivo. Selective role of site-specific phosphorylation. *J. Cell Biol.* 151:1013–1024.

Shah, J.V., L.A. Flanagan, P.A. Janmey, and J.-F. Leterrier. 2000. Bidirectional translocation of neurofilaments along microtubules mediated in part by dynein/dynactin. *Mol. Biol. Cell.* 11:3495–3508.

Shetty, K.T., W.T. Link, and H.C. Pant. 1993. Cdc2-like kinase from rat spinal cord specifically phosphorylates KSPXK motifs in neurofilament proteins: isolation and characterization. *Proc. Natl. Acad. Sci. USA.* 90:6844–6848.

Sun, D., C.L. Leung, and R.K.H. Liem. 1996. Phosphorylation of the high molecular weight neurofilament protein (NF-H) by cdk-5 and p35. *J. Biol. Chem.* 271:14245–14251.

Tu, P.-H., G. Elder, R.A. Lazzarini, D. Nelson, J.Q. Trojanowski, and V.M.-Y. Lee. 1995. Overexpression of the human NFM subunit in transgenic mice modifies the level of endogenous NFL and the phosphorylation state of NFH subunits. *J. Cell Biol.* 129:1629–1640.

Utton, M.A., J. Connell, A.A. Asuni, M. van Slegtenhorst, M. Hutton, R. de Silva, A.J. Lees, C.C. Miller, and B.H. Anderton. 2002. The slow axonal transport of the microtubule-associated protein tau and the transport rates of different isoforms and mutants in cultured neurons. *J. Neurosci.* 22:6394–6400.

Wang, L., and A. Brown. 2001. Rapid intermittent movement of axonal neurofilaments observed by fluorescence photobleaching. *Mol. Biol. Cell.* 12:3257–3267.

Wang, L., C.L. Ho, D. Sun, R.K. Liem, and A. Brown. 2000. Rapid movement of axonal neurofilaments interrupted by prolonged pauses. *Nat. Cell Biol.* 2:137–141.

Yabe, J.S., T. Chylinski, F.-S. Wang, A. Pimenta, S.D. Kattar, M.-D. Linsley, W.K.-H. Chan, and T.B. Shea. 2001. Neurofilaments consist of distinct populations that can be distinguished by C-terminal phosporylation, bundling and axonal transport rates in axonal neurites. *J. Neurosci.* 21:2195–2205.

Yabe, J.T., A. Pimenta, and T.B. Shea. 1999. Kinesin-mediated transport of neurofilament protein oligomers in growing axons. *J. Cell Sci.* 112:3799–3814.

Zhu, Q.Z., M. Lindenbaum, F. Levavasseur, H. Jacomy, and J.P. Julien. 1998. Disruption of the NF-H gene increases axonal microtubule content and velocity of neurofilament transport: relief of axonopathy resulting from the toxin b,b'-iminodipropionitrile. *J. Cell Biol.* 143:183–193.